

Nonadiabatic Potential Energy Surfaces For A Molecule on a Surface as Found by Constrained Complete Active Space Theory

Junhan Chen and Joseph Subotnik*

*Department of Chemistry, University of Pennsylvania, Philadelphia, Pennsylvania 19104,
USA*

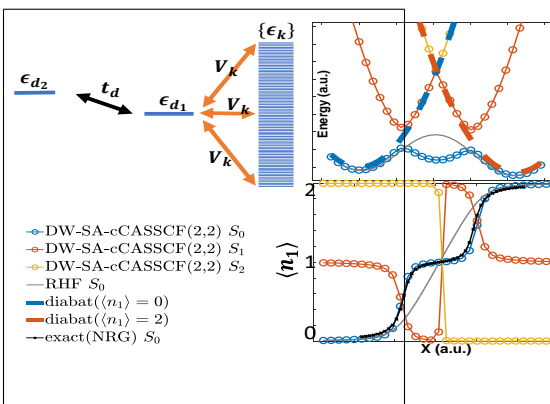
E-mail: subotnik@sas.upenn.edu

Phone: +1 (215) 746-7078

Abstract

In order to study electron-transfer mediated chemical processes on a metal surface, one requires not one but two potential energy surfaces (one ground state and one excited state) as in Marcus theory. In this letter, we report that a novel, dynamically-weighted, state-averaged constrained CASSCF(2,2) (DW-SA-cCASSCF(2,2)) can produce such surfaces for the Anderson Impurity model. Both ground and excited state potentials are smooth, they incorporate states with a charge transfer character, and the accuracy of the ground state surface can be verified for some model problems by renormalization group theory. Future development of gradients and nonadiabatic derivative couplings should allow for the study of non-adiabatic dynamics for molecules near metal surfaces.

Graphical TOC Entry



Keywords

Complete Active Space, State Average, Dynamically Weighting, Metal Surface, Constraint

I Introduction

A great deal of chemistry occurs at interfaces. One can build and run a current through a molecular junction,¹⁻¹⁰ chemisorb and dissociate chemical bonds,¹¹⁻¹⁴ or scatter molecules¹⁵⁻¹⁹ as a few examples. At a microscopic level, the physics underlying these phenomena is much richer and complex than what can be found in solution because of the continuum of electronic states. For instance, to model the phenomena above, one must be able to describe molecular resonance effects on metal surfaces,²⁰ electron-hole-pair quenching,^{11,21} electron-coupled adsorption²² and electron-coupled vibrational motion.^{23,24}

One crucial problem when describing dynamics at metal surfaces is how to model coupled nuclear-electronic motion. Because of the continuum of electronic states at a metal interface, the Born-Oppenheimer approximation can routinely break down¹⁶ and at present, there are far fewer means to model such dynamics (at least relative to dynamics in solution). As originally devised by Suhl,²⁵ the simplest approach for going beyond Born-Oppenheimer at a metal interface is to map all non-Born-Oppenheimer effects into a Markovian “electronic friction” tensor that damps the *nuclear* motion. This approach has been developed by several researchers over the years,²⁶⁻²⁹ and non-Markovian electronic friction tensors have also been proposed. The strength of the electronic friction approach is that, in principle, one runs dynamics along the ground state (or a thermally averaged state) and all information about electronic excited states and nonadiabatic transitions is wrapped into the electronic friction tensor (which can be calculated either within a DFT framework [assuming independent particles]³⁰ or approximated in different ways^{31,32}).

Despite these successes, friction tensors have limitations and have not been able to describe, e.g., the Wodtke charge-transfer experiments.¹⁷ To go beyond these approaches, one would like to run more fully nonadiabatic dynamics at a metal surface, either through an IESH framework³³ or a BCME ansatz;³⁴ note that IESH has been able to model some of the Wodtke experiments (but not all). For these more robust dynamical schemes, however, one must go beyond the ground state and also calculate excited electronic states^{35,36} as well as

the coupling between electronic states. At this point, the electronic structure becomes a real headache as, near a metal surface, there is a continuum of states and one cannot afford to generate too many states; furthermore, with a small or no band gap, it is not immediately obvious how to choose the relevant states.

For extended systems, unfortunately, the traditional high accuracy quantum mechanics methods can be impractical, e.g. coupled-cluster singles, doubles and full triples (CCSDT),^{37,38} second-order perturbation with complete active space (CASPT2)^{39,40} and multireference configuration interaction (MRCI)⁴¹ or full configuration interaction (FCI).^{42,43} If one wishes to calculate excited states for molecules on small clusters or metal surfaces, the standard approaches might include:

1. Constrained DFT (CDFT).^{36,44-47} CDFT has been applied to a few realistic calculations on surface, e.g. charge transport^{48,49} and the energy-level alignment near metal surfaces.⁵⁰ However, the method can fail in the case of strong molecule-metal coupling (i.e. strong hybridization)²⁰ and fractional charge transfer.⁵¹
2. For the specific case of charge transfer, Δ SCF is a powerful tool. One runs two calculations, each with different numbers of electrons. Previous work has successfully modeled at least one case of a molecular resonance near metal surfaces²⁰ with a modified Δ SCF called linear-expansion Δ SCF (and it is believed to be especially relevant in Newns-Anderson-type^{52,53} systems), but it is not clear how to pick linear-expansion coefficients of Kohn-Sham (KS) orbitals for the charge transfer between a molecule and a metal surface; And the nuclear gradient for excited states is very difficult to get.
3. The GW approximation.⁵⁴⁻⁵⁶ One can use many-body theory to extract accurate excitation energies for molecules on clusters. However, these calculations are already expensive and it is difficult to imagine using many-body theory to calculate nonperturbative excited states in such a manner that allows for the calculation of meaningful excited state gradients and derivative couplings.

4. Most powerful of all are embedding methods,^{57–62} which combine high-accuracy quantum chemistry methods with DFT. Embedding approaches have been applied to estimate PESs of excited molecules on clusters⁶³ and surfaces,⁶⁴ but such calculations remain expensive; excited state gradients and derivative couplings will be very costly and charge transfer excited state character is difficult to model.

With this background in mind, over the last few years, our goal has been to construct smooth and qualitatively correct potential energy surfaces for a molecule near a metal surface that should enable us to run non-adiabatic dynamics.^{28,29,65} Because the problem is so difficult—we seek just a *few*, smooth electronic states that can capture the electronic structure of an interacting *continuum* of electrons—one clearly cannot expect quantitative accuracy in all regimes. Ideally, though, one would like a method that can recover both (*i*) the strongly adiabatic limit (where motion along the ground state is a good approximation) and (*ii*) the strongly nonadiabatic limit (where diabatic curves should enter, charge transfer is rare, and Marcus theory applies.) One consequence of this requirement is that the method should work well (*a*) for molecules that are strongly or weakly hybridized (chemisorbed or physisorbed) to a surface, and (*b*) for molecules with strong or weak electron-electron repulsion.

To that end, in the present letter, we will show that a good target approach is to use a dynamically-weighted state-averaged constrained-CASSCF(2,2) (DW-SA-cCASSCF(2,2)). For the famous Anderson-Holstein problem (with one or two sites), we will show that such an ansatz can recover multiple smooth potential energy surfaces, where the ground state roughly matches exact numerical renormalization group theory results (for $U > 0$) or just direct diagonalization (for $U = 0$). We will also show that, without constraints or dynamical weighting, standard CASSCF(2,2) cannot perform nearly as well; in particular, such methods cannot recover smooth curve crossings for the potential energy surfaces. Although DW-SA-cCASSCF(2,2) does fail when more than two electrons becomes strongly entangled (as found, e.g., for certain regimes of a two-site Anderson Impurity model), the data below demonstrates that the method would appear to be an outstanding framework for propagating nonadiabatic

molecular dynamics on metal surfaces in the near future to model charge transfer.

II Theory

When working with extended electronic structure problems, one of the difficulties is extracting accurate (exact) numerical benchmarks. For this reason, when studying embedding problems, one of the most natural Hamiltonians is the Anderson-Holstein (AH) model. Within a second quantized representation, the Hamiltonian can be written as $\hat{H}_{tot} = \hat{H}_{el} - \frac{\hbar^2}{2M} \nabla_x^2$, where the electronic Hamiltonian is:

$$\begin{aligned}
\hat{H}_{el} &= \frac{1}{2}m\omega^2x^2 + \hat{H}_{one}(x) + \hat{\Pi} \\
\hat{H}_{one}(x) &= \epsilon_{d_1}(x) \sum_{\sigma} d_{1\sigma}^{\dagger} d_{1\sigma} + \epsilon_{d_2}(x) \sum_{\sigma} d_{2\sigma}^{\dagger} d_{2\sigma} \\
&+ t_d \sum_{\sigma} (d_{1\sigma}^{\dagger} d_{2\sigma} + d_{2\sigma}^{\dagger} d_{1\sigma}) \\
&+ \sum_{k\sigma} \epsilon_{k\sigma} c_{k\sigma}^{\dagger} c_{k\sigma} + \sum_{k\sigma} V_k (d_{1\sigma}^{\dagger} c_{k\sigma} + c_{k\sigma}^{\dagger} d_{1\sigma}) \\
\hat{\Pi} &= U (d_{1\uparrow}^{\dagger} d_{1\uparrow} d_{1\downarrow}^{\dagger} d_{1\downarrow} + d_{2\uparrow}^{\dagger} d_{2\uparrow} d_{2\downarrow}^{\dagger} d_{2\downarrow}) \\
\epsilon_{d_1}(x) &= e_{d_1} - \sqrt{2}gx \\
\epsilon_{d_2}(x) &= e_{d_2} - \sqrt{2}gx
\end{aligned} \tag{1}$$

In this paper, we will not consider nuclear motion and will focus on treating the electronic Hamiltonian, \hat{H}_{el} ; the parameter x will be a constant that we can vary for each calculation below (the term $\frac{1}{2}m\omega^2x^2$ representing the potential energy of a nuclear vibration associated with the molecule or impurity). The operators $\{\hat{d}_1^{\dagger}, \hat{d}_2^{\dagger}\}$ create impurity atomic orbitals, the operators \hat{c}_k^{\dagger} create bath (metal surface) atomic orbitals, and σ denotes an electron spin. $\epsilon_{d_1}(x)$ and $\epsilon_{d_2}(x)$ are one-electron ionization energies for the impurities (which linearly depend on the impurity nuclear coordinate x); ϵ_k denotes the energy of bath orbital k . t_d is the hopping parameter between site 1 and site 2, U represents the on-site coulomb repulsion

for the impurity. V_k represents the hybridization between impurity site 1 and the metal bath, and as in the wide band approximation, is characterized by:

$$\Gamma = \Gamma(\epsilon) = 2\pi \sum_k |V_k|^2 \delta(\epsilon - \epsilon_k), \quad (2)$$

where Γ is assumed to be constant through the whole energy spectrum ϵ .

The difficulty in solving the interfacial electronic structure theory with a metallic solid arises from the low-lying electron-hole-pair excitation within the metal, whose excitation energy is negligibly small; for interfacial problems, there is a true continuum of states and there is no gap between the ground and first excited state. This state of affairs contrasts with the case of an isolated molecule, where the potential energy surfaces are usually well-separated for most of nuclear configuration space with only a few crossings at isolated geometries. Moreover, as discussed above, for problems with charge transfer, we require both ground and excited states and ideally the capacity to diabatically connect the two sets of manifolds; alas standard diabaticization schemes^{66,67} are not directly applicable in this case.

With this background in mind, we have sought to explore whether standard (but slightly tweaked) quantum chemistry methods can solve such interface problem, in particular CASSCF-like solutions. Our recent forays into different versions of Hartree-Fock theory with non-orthogonal orbitals [partially-optimized closed-or-open-shell Hartree-Fock (poCOOS-HF)⁶⁸] have pointed to CASSCF(2,2) as the most natural (and improved) starting point. To that end, we will explore four different CASSCF-based approaches for modeling the AH model:

1. Standard complete active space self-consistent-field (CASSCF). We will show that this approach works well for capturing static correlation and an accurate ground state energy. However, not surprisingly for the CASSCF experts, the method can yield incorrect ground-excited state gaps/crossings with discontinuous surfaces.
2. Dynamically weighted state-averaged CASSCF (DW-SA-CASSCF). State-averaging can fix many of the discontinuities of CASSCF, though at the expense of less accu-

rate ground state energies (again, not surprising to a CASSCF expert). In practice, dynamical-weighting (DW) usually outperforms static weighting as far as achieving a better balance between accurate energies and continuous surfaces; dynamic weighting can avoid some of the usual pitfalls of static state-averaged CASSCF (e.g., example, the unnecessary discontinuities in the excited state energy surfaces as found for butadiene twisting;⁶⁹ or the incorrect avoided crossing geometries as found with Li-F⁷⁰). Our dynamical weighting scheme follows Ref.⁷⁰ Unfortunately, despite these improvements, we will find that DW-SA-CASSCF can still fail for the AH model because one cannot always isolate a consistent set of electronic states with meaningful impurity character; the intruder problem remains a nightmare.

3. Constrained CASSCF (cCASSCF). Our experience above will lead us to the concept of a *constrained* CASSCF (cCASSCF) optimization procedure, whereby we insist that the molecular population in the active space (spanned by active orbitals $\{t, u\}$) always has magnitude equal to unity:

$$\sum_{\mu \in \text{impurity}} \langle t | d_{\mu}^{\dagger} d_{\mu} | t \rangle + \langle u | d_{\mu}^{\dagger} d_{\mu} | u \rangle = 1 \quad (3)$$

This approach helps with the intruder state problem, but excited states can still be discontinuous far away from the crossing regime.

4. Dynamically Weighted State-averaged constrained CASSCF (DW-SA-cCASSCF). Our best overall candidate for exploring excited state dynamics at an interface, with accurate electronic energies and smooth surfaces, combines both the dynamical weighting and the impurity constraint to definitively solve the intruder state problem for the AH model.

For a complete description of the relevant theory and all of the relevant equations needed to define and implement these methods, please see Ref.⁷¹

III Results

As discussed above, a meaningful electronic structure description of a molecular dynamics on a metal surface surface should be accurate both in the weak and strong coupling limits, and in the limits of strong and weak electron-electron repulsion. Because we do not run dynamics here, we cannot check the first condition (Γ/ω big or small). However, we can check the second condition (U/Γ). Below, we will work with a manifold of electronic states for which the wide-band approximation holds. An investigation of different values for U indicates that DW-SA-cCASSCF(2,2) has a great deal of promise.

A $U = 0$, one-site Hamiltonian

We begin with the case $U = 0$, for which an exact solution can be constructed (as there is no electron-electron correlation). In Figs. 1(a,b), we plot the energy and the electron population as a function of the nuclear coordinate x for traditional state-specific CASSCF(2,2). We find immediately that the method generates three nearly degenerate states. One would hypothesize that the two active orbitals do not have any impurity character and the excited states have metal-to-metal excitation character on top of the ground state. This suspicion is confirmed in Fig. 1(b) showing that the electron population behavior for the ground and excited states are nearly the same.

Clearly, state-specific CASSCF(2,2) cannot consistently generate the two active orbitals that have any impurity character and thus cannot model charge transfer. To avoid the scenario of Figs. 1(a,b), the 2 active orbitals t, u should be a mixture of impurity atomic orbitals $\{d_\mu\}$ and bath atomic orbitals $\{b_\nu\}$ (and not just bath orbitals). This conclusion leads to the constraint in Eq. 3. In Ref.,⁷¹ we derive in detail the necessary equations that must be implemented in order to solve CASSCF(2,2) with such a constraint. In short, one can integrate a standard CASSCF routine within a Lagrange multiplier self-consistently loop.

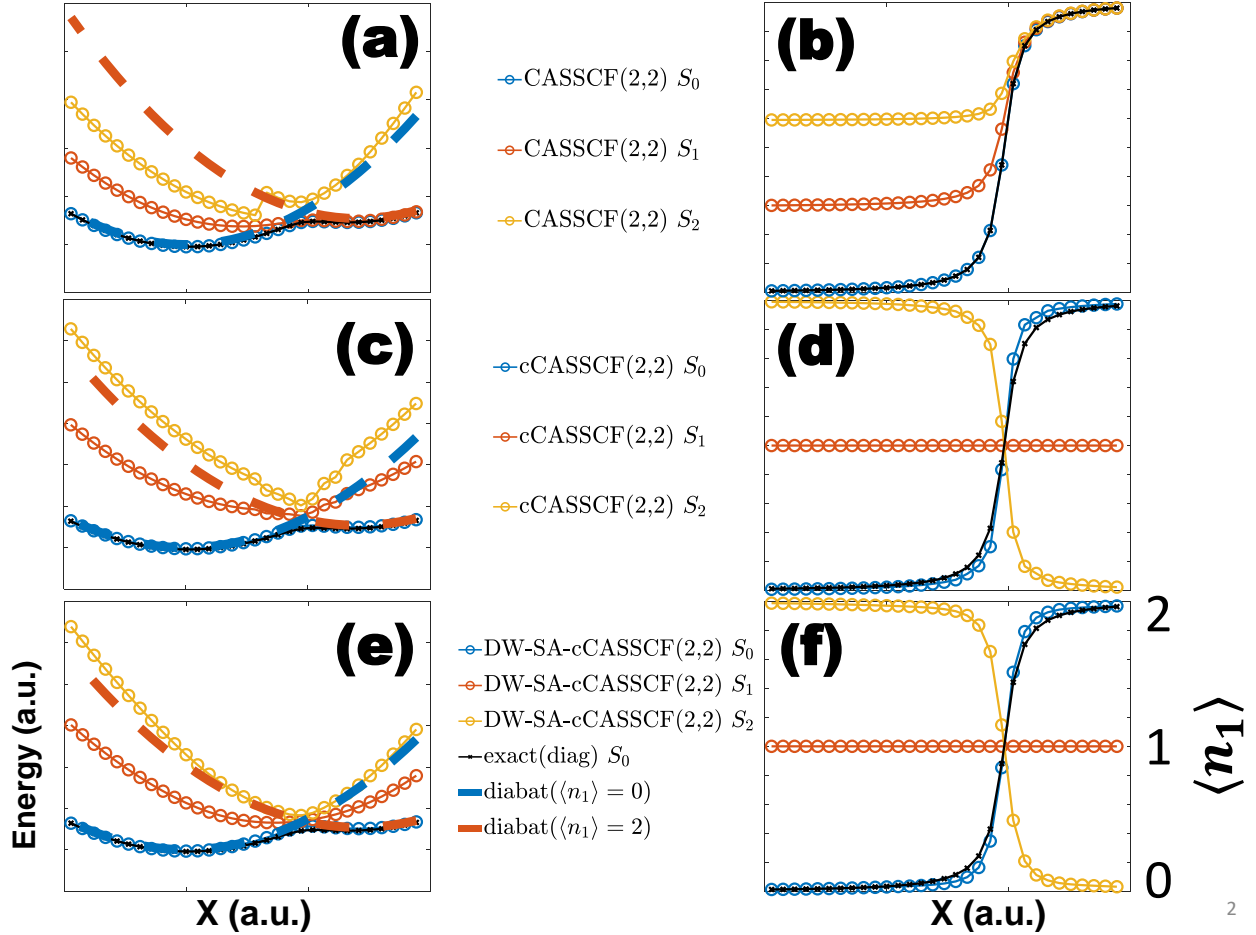


Figure 1: The energies and the impurity electron population ($\langle n_1 \rangle$) of the 1-site Anderson impurity model *without* electron-electron repulsion for three CASSCF(2,2) methods: (a,b) CASSCF(2,2); (c,d) Constrained CASSCF(2,2) (cCASSCF(2,2)); (e,f) Dynamical-weighted state-averaged constrained CASSCF(2,2) (DW-SA-cCASSCF(2,2)) with $\zeta = 40$. On the right hand side, the black line is the exact adiabatic ground state energy and electron populations (by direct diagonalization) and two dashed lines represent two exact diabatic energies with $\langle n_1 \rangle = 0$ and $\langle n_1 \rangle = 2$. Note that CASSCF(2,2) and cCASSCF(2,2) excited state energies do not agree in (a,c) because there are so many states around to choose from. The parameter set is $m\omega^2 = 0.003$, $g = 0.0075$, $e_{d_1} = 0.05$, $\Gamma = 0.01$, $U = 0$ with 101 metal states evenly distributed within the energy window $[-0.05, 0.05]$.

In Figs. 1(c,d), we plot results for constrained CASSCF(2,2). As one would hope, now we do see the desired electron population behavior (three curves crossing) in Fig. 1(d). However, note that the constrained CASSCF(2,2) excited state energies do have a small discontinuity; moreover, these energies not ever reach the proper diabatic limit when the impurity is fully occupied ($\langle n_1 \rangle = 2$) or totally unoccupied ($\langle n_1 \rangle = 0$). At bottom, the problem is that, if one optimizes only the ground state energy (and pays no attention to the excited state energies), one risks having inaccurate excited states (a standard feature of CASSCF solutions). Moreover, for this specific problem ($U = 0$), no active space is needed for exact diagonalization, and so the excited state energies are not even well defined. Visually, this failure becomes most acute far away from the curve crossing, where the S_2 excited state energy is quite different from the diabatic energy $diabat(\langle n_1 \rangle = 2)$ on the right hand side and the diabatic energy $diabat(\langle n_1 \rangle = 0)$ on the left hand side.

Finally, in Figs. 1(e,f), we plot results for dynamically-weighted state-averaged constrained CASSCF(2,2). This method appears to give the best of both worlds: an accurate ground states and smooth excited states with the right asymptotic limits. The method succeeds by smoothly interpolating the fock operator between state-specific and state-averaged regime, while still enforcing the constraint that the impurity must be involved.

B $U > 0$, one-site and two-site Hamiltonian

Having explored three CASSCF(2,2) methods for 1-site Anderson model *without* the electron-electron repulsion, we will now address the 1-site and 2-site Anderson models *with* electron-electron repulsion, which is more realistic and more difficult to solve.

B.1 One Site

In the Fig. 2, we plot results for the 1-site model *with* the electron-electron repulsion according to the CASSCF(2,2) methods discussed above. Although one cannot recover the exact ground state energy for this entangled Hamiltonian, one can extract the exact impurity

population using numerical renormalization group theory (NRG).^{72,73}

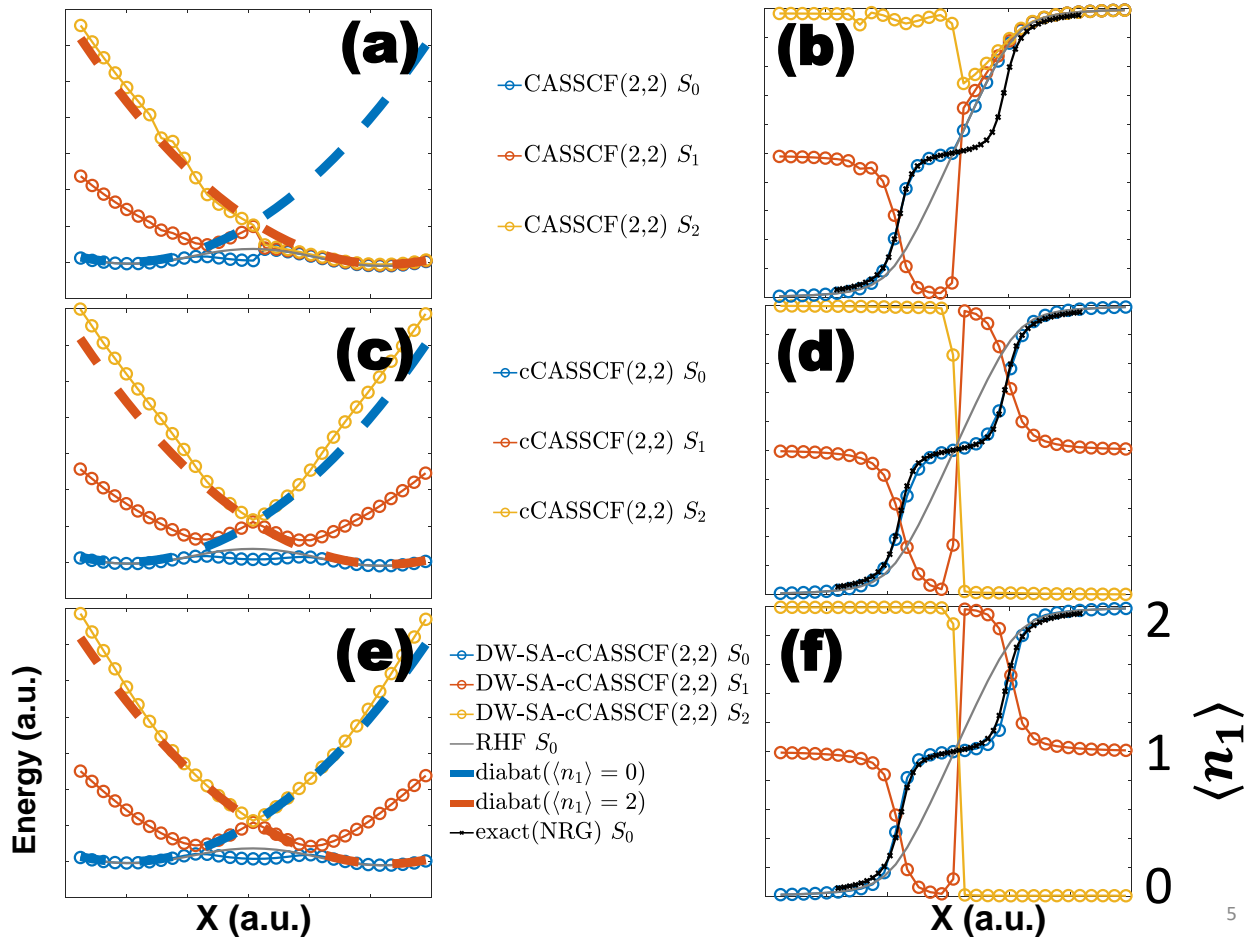


Figure 2: The energies and the impurity electron population ($\langle n_1 \rangle$) of the 1-site Anderson impurity model *with* electron-electron repulsion for three CASSCF(2,2) methods: (a,b) CASSCF(2,2); (c,d) Constrained CASSCF(2,2) (cCASSCF(2,2)); (e,f) Dynamical-weighted state-averaged constrained CASSCF(2,2) (DW-SA-cCASSCF(2,2)) with $\zeta = 40$. On the right hand side, the black line is the exact adiabatic ground state electron population (calculated by numerical renormalization group, NRG) and two dashed lines represent two exact diabatic energies with $\langle n_1 \rangle = 0$ and $\langle n_1 \rangle = 2$. The blue line without the circle is the RHF energy and electron populations. Note that *with* the electron-electron repulsion, DW-SA-cCASSCF(2,2) can produce a triple energy well corresponding to $\langle n_1 \rangle = 0, \langle n_1 \rangle = 1, \langle n_1 \rangle = 2$ while RHF is qualitatively wrong. The parameter set is $m\omega^2 = 0.001, g = 0.0075, e_{d_1} = 0.06, \Gamma = 0.01, U = 0.1$ with 101 metal states evenly distributed within the energy window $[-0.05, 0.05]$.

According to Fig. 2, our conclusions with $U > 0$ are largely the same as our conclusions with $U = 0$. In both cases, DW-SA-cCASSCF(2,2) would appear to offer the best compromise between an accurate ground state and smooth excited states with the correct asymptotic limits. Note that, when $U > 0$ (unlike when $U = 0$), we find not one but two

excited state crossings as the zero-to-one and one-to-two electron transitions are no longer on top of each other.

B.2 Two Sites

Lastly, the results above might appear artificial in the sense that there is only one impurity orbital. After all, according to the constraint in Eqn. 3, there is much less flexibility than one will find in a model with more than one site (and multiple impurity orbitals). To that end, in Fig. 3, we plot the energy and electron population results according DW-SA-cCASSCF(2,2) for a 2-site model *with* electron-electron repulsion. We explore both the limit where the impurities are strongly-bound together (large t_d , Figs. 3 (a,b)) or weakly-bound together (small t_d , Figs. 3 (c,d)). We explore a large range of possible impurity energies with two independent electron transfer events.

For the strong-bound limit, in Fig. 3(a,b), we see that DW-SA-cCASSCF(2,2) again performs well, recovering reasonably accurate impurity populations over the regime where the impurity is occupied by two or three or four electrons. However, in the weakly-bound limit (Fig. 3 (d)), we do find some qualitative errors. While DW-SA-cCASSCF(2,2) can capture an accurate ground state as the impurity population switches from four to three electrons, the electron population fails to match with NRG as the population switches from three to two electrons. In this regime, it would appear that there need to be several unpaired electrons, as we have both an electron transfer and a bond-breaking event simultaneously; apparently, an active space of 2 electrons and 2 orbitals is not large enough to fully account for such a process. In principle, one should be able to improve these results either by increasing the active size or performing a configuration interaction on top of the CASSCF(2,2) reference states. These approaches will be taken up in a future paper.

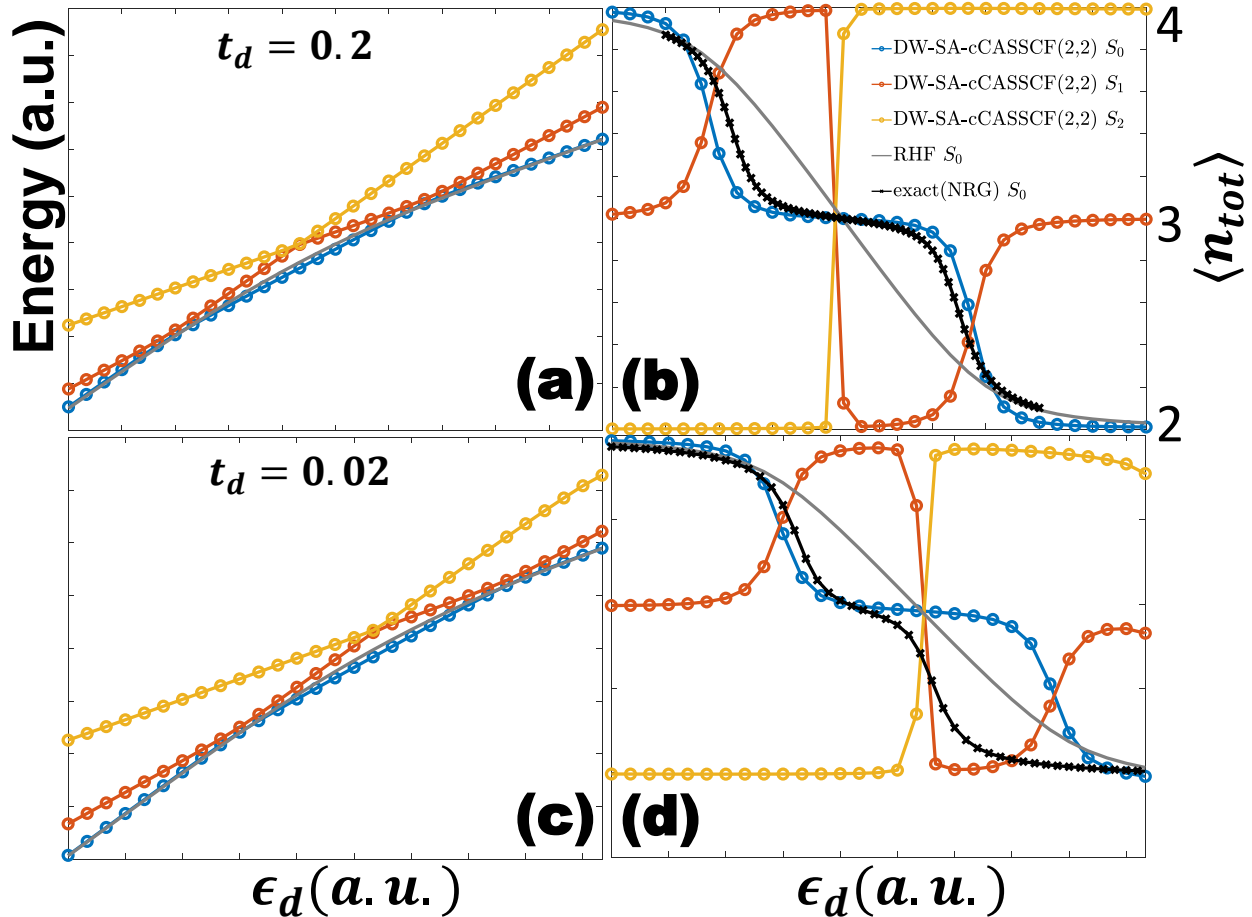


Figure 3: The energies and the impurity electron population ($\langle n_{tot} \rangle$) of the 2-site Anderson impurity model *with* electron-electron repulsion for dynamical-weighted state-averaged constrained CASSCF(2,2) (DW-SA-cCASSCF(2,2)) with $\zeta = 40$. (a) Strong-bonded case with $t_d = 0.2$; (b) Weak-bonded case with $t_d = 0.02$. Subfigures (a,c) don't include the harmonic nuclear potentials. On the right hand side, the black line is the exact adiabatic ground state electron population (calculated by numerical renormalization group, NRG). The blue line without the circle is the RHF energy and electron populations. In general, DW-SA-cCASSCF(2,2) performs well but the method fails to match NRG in the weak-bonded $t_d = 0.02$ limit for the ground state electron population (as a bigger active space is likely required). The parameter set is $\epsilon_{d_1} = \epsilon_{d_2}, \Gamma = 0.01, U = 0.1$ with 101 metal states evenly distributed within the energy window $[-0.05, 0.05]$.

IV Discussion: The Choice of Constraint

Our results above have highlighted the power of a constrained dynamically weighted state-averaged CASSCF(2,2) calculation so as to model a molecule on a surface. In order to run *ab initio* molecular dynamics on a metal surface, however, quite a few more topics will need

to be explored and made more efficient, as we will now discuss.

The first and most glaring omission in the present letter are the timings or computational cost of the present algorithm. For the most part, the present calculations were coded in a fairly inefficient manner, requiring on the order of minutes for completion. Future work will need to benchmark these timings and investigate the best optimization routine so as to minimize them. Second, in order to run nonadiabatic dynamics at a metal surface (as opposed to the case of solution), one will require couplings to the metal surface (capturing electronic motion in the absence of nuclear motion). These couplings will be reported in a future publication. Third, in this letter, we have not investigated how our results depend on the dynamical-weighting factor ζ . This too will be reported in a future publication. Fourth, in practice, it will be crucial to extract gradients, derivative couplings, and diabatic states from the present ansatz. All of these features will be essential if we are to eventually run *ab initio* simulations.

Fifth and finally, although we have shown in this letter why implementing a constraint can be crucial when applying CASSCF to the case of a molecule on a metals surface, we have not demonstrated that the constraint in Eq. 3 is actually optimal. In particular, one can easily imagine replacing Eq. 3 (where two active orbitals have some overlap with the impurity atomic orbitals) with a fully localized constraint (where we force each orbital to be either on the molecule or in the metal). Mathematically, one can imagine replacing Eq. 3 (which we might call a partially localized constraint pcCASSCF(2,2)) with the fully localized constraint (which we might call a fully localized constraint fcCASSCF(2,2)) in Eq. 4:

$$\begin{aligned} \sum_{\mu \in \text{impurity}} \langle t | d_{\mu}^{\dagger} d_{\mu} | t \rangle &= 1; \\ \sum_{\mu \in \text{impurity}} \langle u | d_{\mu}^{\dagger} d_{\mu} | u \rangle &= 0 \end{aligned} \tag{4}$$

Differentiating between these two constraint frameworks is essential for understanding how best to understand and conceptualize how electron correlation functions a metal surface.

After all, Eq. 4 is just about the simplest framework one can imagine implementing for modeling electron transfer—the equivalent of standard constrained DFT but for CASSCF. What are practical differences between these two constraints?

Now, it is important to emphasize that, in the single-impurity case, these two constraints are equivalent. Suppose $\{t, u\}$ are two active orbitals solved by pcCASSCF(2,2). For any CASSCF solution, the wavefunction is invariant by the unitary rotation within the active space, which provides one degree of freedom (the rotation angle θ) to formulate a set of new active orbitals $\{t', u'\}$:

$$\begin{aligned} |t'\rangle &= \cos(\theta) |t\rangle + \sin(\theta) |u\rangle \\ |u'\rangle &= \sin(\theta) |t\rangle - \cos(\theta) |u\rangle \end{aligned} \tag{5}$$

In single impurity case, the rotation angle θ can be chosen to satisfy:⁷⁴ $|\langle d|t'\rangle|^2 = 1$, where d represents the impurity atomic orbital, and using the fact that $|\langle d|t'\rangle|^2 + |\langle d|u'\rangle|^2 = 1$, it follows that $|\langle d|u'\rangle|^2 = 0$. Thus, for a single state impurity, fcCASSCF(2,2) and pcCASSCF(2,2) are equivalent. However, this statement no longer holds for multi-impurity case, e.g. two-impurity case, because we are not guaranteed to find a θ to satisfy:⁷⁵

$$|\langle d_1|t'\rangle|^2 + |\langle d_2|t'\rangle|^2 = 1 \tag{6}$$

To that end, we have coded up and compared Eq. 3 vs. Eq. 4. Our results for the two-site model are shown in Fig. 4. In Fig. 4(a), we find that the pcCASSCF(2,2) results are inversion symmetric around the point $(\epsilon_d, \langle n_{tot} \rangle) = (0, 2)$. This inversion symmetry can be understood as a diabatic crossing between the diabat($\langle n_{tot} \rangle = 3$) and the diabat($\langle n_{tot} \rangle = 1$) for S_1 (or between the diabat($\langle n_{tot} \rangle = 4$) and the diabat($\langle n_{tot} \rangle = 0$) for S_2); pcCASSCF(2,2) captures these transition smoothly. By contrast, we find that the fcCASSCF(2,2) results are not inversion symmetric and there is a discontinuity at $\epsilon_d = 0.02$, indicating that there can be multiple solutions in the regime $\epsilon_d \in (-0.025, 0.02)$. The energetic results shown Fig. 4(b) also support this observation. In the end, the evidence would suggest that fcCASSCF(2,2)

will suffer a more serious multiple solution problem (and exhibit more discontinuities) than does pcCASSCF. Thus, we must conclude that the latter is indeed a better starting point than the former as far as running dynamics.

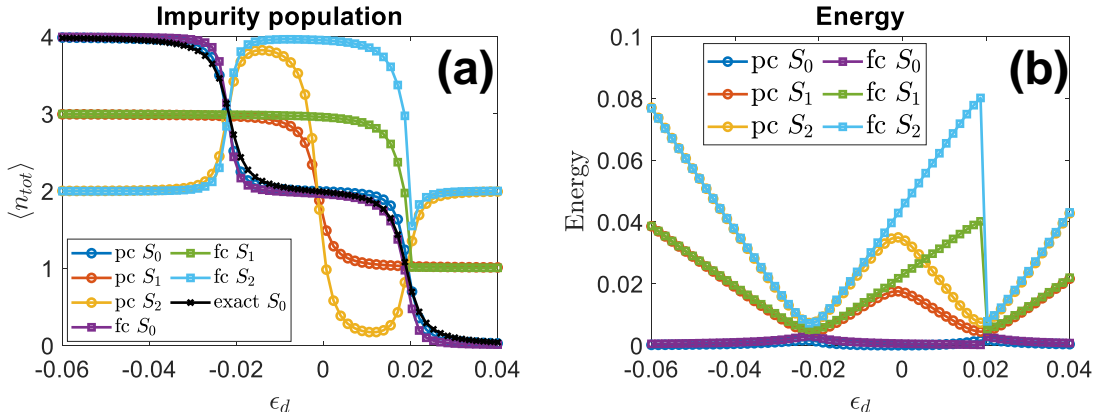


Figure 4: Comparison of partially localized constraint (pc for DW-SA-pcCASSCF(2,2)) and fully localized constraint (fc for DW-SA-fcCASSCF(2,2)). (a) Electron populations; (b) Energies (relative to exact). Note that DW-SA-fcCASSCF(2,2) suffers the multiple solution problem (the cause of the discontinuity at $\epsilon_d = 0.02$); the partial constraint is smoother and more robust. The parameter set is: $\epsilon_d = \epsilon_{d_1} = \epsilon_{d_2}$, $\Gamma = 0.01$, $U = 0$, $t_d = 0.02$, $\zeta = 40$ with 31 metal states evenly distributed within the energy window $[-0.015, 0.015]$.

V Conclusion

In conclusion, in this letter, we have reported a modified CASSCF(2,2) method, dynamically-weighted state-averaged constrained CASSCF(2,2) (DW-SA-cCASSCF(2,2)), which can generate smooth crossings and demonstrably accurate ground states for simple molecules near metal surfaces; inclusion of a constraint is essential for picking out the relevant manifold of states and dynamical weighting is key for ensuring the smoothness. While the accuracy of this approach will no doubt be limited when larger molecules (with more electron correlation) are studied, one can hope that this approach will be able to offer some qualitative accuracy at the least to a very difficult problem where few nonadiabatic effects have been investigated in detail (though see recent work of Levine *et al* for an interesting CAS calculation of dangling bonds on a silicon cluster).⁷⁶ One can also imagine expanding the present method to

much larger active spaces in the spirit of heat bath configuration interaction self-consistent field (HCISCF),⁷⁷ where nuclear gradients are now available.

Looking forward, two potential directions would be very exciting to explore in the future. First, armed with a set of well-defined ground state and excited states, one could very much like to study nonadiabatic dynamics directly and observe how both nuclear motion and bath-induced electronic relaxation in the metal contribute (and potentially compete) when molecules vibrate in the presence of a continuum of electronic states. To that end, we are in the process now of implementing the fewest-switches-surface-hopping with electron-relaxation (FSSH-ER) algorithm⁶⁵ to study the Anderson model *with* the electron-electron correlation effect, which represents a more realistic model for molecules near metal surfaces. Second, in the future, it will be very interesting to adapt the present DW-SA-cCASSCF(2,2) method to an *ab initio* electronic structure package, so that we can make concrete predictions about realistic molecules that are bound to a metallic surface and then oxidized or reduced. If successful, this approach should make contact with a range of both inner and outer sphere electrochemical experiments, allowing us to probe questions about the adiabaticity or nonadiabaticity of such processes ; answers to these questions as of yet are still largely unknown.

Acknowledgement

This work was supported by the U.S. Air Force Office of Scientific Research (USAFOSR) under Grant Nos. FA9550-18-1-0497 and FA9550-18-1-0420. We thank the DoD High Performance Computing Modernization Program for computer time. We thank Xuezhi Bian for helpful discussions regarding state-averaged CASSCF. We also thank Yanze Wu for helpful discussions regarding the nuclear degrees of freedom in the one-site Anderson Impurity model *with* electron-electron repulsion.

Supporting Information Available

This will usually read something like: “Experimental procedures and characterization data for all new compounds. The class will automatically add a sentence pointing to the information on-line:

References

- (1) Alemani, M.; Peters, M. V.; Hecht, S.; Rieder, K.-H.; Moresco, F.; Grill, L. Electric field-induced isomerization of azobenzene by STM. *Journal of the American Chemical Society* **2006**, *128*, 14446–14447.
- (2) Danilov, A. V.; Kubatkin, S. E.; Kafanov, S. G.; Flensberg, K.; Bjørnholm, T. Electron transfer dynamics of bistable single-molecule junctions. *Nano letters* **2006**, *6*, 2184–2190.
- (3) Donarini, A.; Grifoni, M.; Richter, K. Dynamical symmetry breaking in transport through molecules. *Physical review letters* **2006**, *97*, 166801.
- (4) Henningsen, N.; Franke, K.; Torrente, I.; Schulze, G.; Prievisch, B.; Rück-Braun, K.; Dokić, J.; Klamroth, T.; Saalfrank, P.; Pascual, J. Inducing the rotation of a single phenyl ring with tunneling electrons. *The Journal of Physical Chemistry C* **2007**, *111*, 14843–14848.
- (5) Datta, S.; Tian, W.; Hong, S.; Reifenberger, R.; Henderson, J. I.; Kubiak, C. P. Current-voltage characteristics of self-assembled monolayers by scanning tunneling microscopy. *Physical Review Letters* **1997**, *79*, 2530.
- (6) Samanta, M.; Tian, W.; Datta, S.; Henderson, J.; Kubiak, C. Electronic conduction through organic molecules. *Physical review B* **1996**, *53*, R7626.

- (7) Nitzan, A.; Ratner, M. A. Electron transport in molecular wire junctions. *Science* **2003**, *300*, 1384–1389.
- (8) Mujica, V.; Kemp, M.; Roitberg, A.; Ratner, M. Current-voltage characteristics of molecular wires: Eigenvalue staircase, Coulomb blockade, and rectification. *The Journal of chemical physics* **1996**, *104*, 7296–7305.
- (9) Hsu, C.-P.; Marcus, R. A sequential formula for electronic coupling in long range bridge-assisted electron transfer: Formulation of theory and application to alkanethiol monolayers. *The Journal of chemical physics* **1997**, *106*, 584–598.
- (10) Stipe, B. C.; Rezaei, M. A.; Ho, W. Single-molecule vibrational spectroscopy and microscopy. *Science* **1998**, *280*, 1732–1735.
- (11) Jiang, B.; Alducin, M.; Guo, H. Electron–hole pair effects in polyatomic dissociative chemisorption: Water on Ni (111). *The Journal of Physical Chemistry Letters* **2016**, *7*, 327–331.
- (12) Maurer, R. J.; Jiang, B.; Guo, H.; Tully, J. C. Mode specific electronic friction in dissociative chemisorption on metal surfaces: H₂ on Ag (111). *Physical review letters* **2017**, *118*, 256001.
- (13) Yin, R.; Zhang, Y.; Libisch, F.; Carter, E. A.; Guo, H.; Jiang, B. Dissociative chemisorption of O₂ on Al (111): dynamics on a correlated wave-function-based potential energy surface. *The journal of physical chemistry letters* **2018**, *9*, 3271–3277.
- (14) Chen, J.; Zhou, X.; Zhang, Y.; Jiang, B. Vibrational control of selective bond cleavage in dissociative chemisorption of methanol on Cu (111). *Nature communications* **2018**, *9*, 1–7.
- (15) Waldeck, D.; Alivisatos, A.; Harris, C. Nonradiative damping of molecular electronic excited states by metal surfaces. *Surface Science* **1985**, *158*, 103–125.

- (16) Wodtke*, A. M.; Tully, J. C.; Auerbach, D. J. Electronically non-adiabatic interactions of molecules at metal surfaces: Can we trust the Born–Oppenheimer approximation for surface chemistry? *International Reviews in Physical Chemistry* **2004**, *23*, 513–539.
- (17) Bartels, C.; Cooper, R.; Auerbach, D. J.; Wodtke, A. M. Energy transfer at metal surfaces: the need to go beyond the electronic friction picture. *Chemical Science* **2011**, *2*, 1647–1655.
- (18) Kandratsenka, A.; Jiang, H.; Dorenkamp, Y.; Janke, S. M.; Kammler, M.; Wodtke, A. M.; Bünermann, O. Unified description of H-atom–induced chemi-currents and inelastic scattering. *Proceedings of the National Academy of Sciences* **2018**, *115*, 680–684.
- (19) Shenvi, N.; Roy, S.; Tully, J. C. Dynamical steering and electronic excitation in NO scattering from a gold surface. *Science* **2009**, *326*, 829–832.
- (20) Gavnholt, J.; Olsen, T.; Englund, M.; Schiøtz, J. Δ self-consistent field method to obtain potential energy surfaces of excited molecules on surfaces. *Physical Review B* **2008**, *78*, 075441.
- (21) Persson, B.; Lang, N. Electron-hole-pair quenching of excited states near a metal. *Physical Review B* **1982**, *26*, 5409.
- (22) Bünermann, O.; Jiang, H.; Dorenkamp, Y.; Kandratsenka, A.; Janke, S. M.; Auerbach, D. J.; Wodtke, A. M. Electron-hole pair excitation determines the mechanism of hydrogen atom adsorption. *Science* **2015**, *350*, 1346–1349.
- (23) Morin, M.; Levinos, N.; Harris, A. Vibrational energy transfer of CO/Cu (100): Non-adiabatic vibration/electron coupling. *The Journal of Chemical Physics* **1992**, *96*, 3950–3956.

- (24) Huang, Y.; Rettner, C. T.; Auerbach, D. J.; Wodtke, A. M. Vibrational promotion of electron transfer. *Science* **2000**, *290*, 111–114.
- (25) d’Agliano, E. G.; Kumar, P.; Schaich, W.; Suhl, H. Brownian motion model of the interactions between chemical species and metallic electrons: Bootstrap derivation and parameter evaluation. *Physical Review B* **1975**, *11*, 2122.
- (26) Bohnen, K.-P.; Kiwi, M.; Suhl, H. Friction Coefficient of an Adsorbed H Atom on a Metal Surface. *Physical Review Letters* **1975**, *34*, 1512.
- (27) Brandbyge, M.; Hedegård, P.; Heinz, T.; Misewich, J.; Newns, D. Electronically driven adsorbate excitation mechanism in femtosecond-pulse laser desorption. *Physical Review B* **1995**, *52*, 6042.
- (28) Jin, Z.; Subotnik, J. E. A practical ansatz for evaluating the electronic friction tensor accurately, efficiently, and in a nearly black-box format. *The Journal of Chemical Physics* **2019**, *150*, 164105.
- (29) Dou, W.; Subotnik, J. E. Perspective: How to understand electronic friction. *The Journal of Chemical Physics* **2018**, *148*, 230901.
- (30) Maurer, R. J.; Askerka, M.; Batista, V. S.; Tully, J. C. Ab initio tensorial electronic friction for molecules on metal surfaces: Nonadiabatic vibrational relaxation. *Physical Review B* **2016**, *94*, 115432.
- (31) Rittmeyer, S. P.; Meyer, J.; Juaristi, J. I.; Reuter, K. Electronic friction-based vibrational lifetimes of molecular adsorbates: Beyond the independent-atom approximation. *Physical review letters* **2015**, *115*, 046102.
- (32) Juaristi, J. I.; Alducin, M.; Muiño, R. D.; Busnengo, H. F.; Salin, A. Role of Electron-Hole Pair Excitations in the Dissociative Adsorption of Diatomic Molecules on Metal Surfaces. **2008**, *100*, 116102.

- (33) Shenvi, N.; Roy, S.; Tully, J. C. Nonadiabatic dynamics at metal surfaces: Independent-electron surface hopping. *The Journal of chemical physics* **2009**, *130*, 174107.
- (34) Dou, W.; Subotnik, J. E. A broadened classical master equation approach for nonadiabatic dynamics at metal surfaces: Beyond the weak molecule-metal coupling limit. *The Journal of chemical physics* **2016**, *144*, 024116.
- (35) Lichten, W. Resonant charge exchange in atomic collisions. *Physical Review* **1963**, *131*, 229.
- (36) Behler, J.; Delley, B.; Reuter, K.; Scheffler, M. Nonadiabatic potential-energy surfaces by constrained density-functional theory. *Physical Review B* **2007**, *75*, 115409.
- (37) Raghavachari, K.; Trucks, G. W.; Pople, J. A.; Head-Gordon, M. A fifth-order perturbation comparison of electron correlation theories. *Chemical Physics Letters* **1989**, *157*, 479–483.
- (38) Crawford, T. D.; Schaefer III, H. F. An introduction to coupled cluster theory for computational chemists. *Reviews in computational chemistry* **2007**, *14*, 33–136.
- (39) Andersson, K.; ÅA, P. P.-. Malmqvist, BO Roos, AJ Sadlej, K. Wolinski. *J. Phys. Chem* **1990**, *94*, 5483.
- (40) Andersson, K.; Malmqvist, P.-Å.; Roos, B. O. Second-order perturbation theory with a complete active space self-consistent field reference function. *The Journal of chemical physics* **1992**, *96*, 1218–1226.
- (41) Bruna, P.; Peyerimhoff, S. Excited-state potentials. *Ab initio methods in quantum chemistry, I* **1987**, 1–98.
- (42) Sherrill, C. D.; Schaefer III, H. F. *Advances in quantum chemistry*; Elsevier, 1999; Vol. 34; pp 143–269.

- (43) Sherrill, C. D. *Computational algorithms for large-scale full and multi-reference configuration interaction wavefunctions*; University of Georgia, 1996.
- (44) Wu, Q.; Van Voorhis, T. Extracting electron transfer coupling elements from constrained density functional theory. *The Journal of chemical physics* **2006**, *125*, 164105.
- (45) Wu, Q.; Van Voorhis, T. Direct optimization method to study constrained systems within density-functional theory. *Physical Review A* **2005**, *72*, 024502.
- (46) Kaduk, B.; Kowalczyk, T.; Van Voorhis, T. Constrained density functional theory. *Chemical Reviews* **2012**, *112*, 321–370.
- (47) Meng, G.; Jiang, B. A pragmatic protocol for determining charge transfer states of molecules at metal surfaces by constrained density functional theory. *The Journal of Chemical Physics* **2022**, *157*, 214103.
- (48) Goldey, M. B.; Brawand, N. P.; Voros, M.; Galli, G. Charge transport in nanostructured materials: implementation and verification of constrained density functional theory. *Journal of chemical theory and computation* **2017**, *13*, 2581–2590.
- (49) Ma, H.; Wang, W.; Kim, S.; Cheng, M.-H.; Govoni, M.; Galli, G. PyCDFT: A Python package for constrained density functional theory. *Journal of Computational Chemistry* **2020**,
- (50) Souza, A.; Rungger, I.; Pemmaraju, C.; Schwingenschlögl, U.; Sanvito, S. Constrained-DFT method for accurate energy-level alignment of metal/molecule interfaces. *Physical Review B* **2013**, *88*, 165112.
- (51) Mavros, M. G.; Van Voorhis, T. Communication: CDFT-CI couplings can be unreliable when there is fractional charge transfer. *The Journal of Chemical Physics* **2015**, *143*, 231102.

- (52) Newns, D. Self-consistent model of hydrogen chemisorption. *Physical Review* **1969**, *178*, 1123.
- (53) Anderson, P. W. Localized magnetic states in metals. *Physical Review* **1961**, *124*, 41.
- (54) Hedin, L. New method for calculating the one-particle Green's function with application to the electron-gas problem. *Physical Review* **1965**, *139*, A796.
- (55) Onida, G.; Reining, L.; Rubio, A. Electronic excitations: density-functional versus many-body Green's-function approaches. *Reviews of modern physics* **2002**, *74*, 601.
- (56) Liu, Z.-F.; da Jornada, F. H.; Louie, S. G.; Neaton, J. B. Accelerating GW-based energy level alignment calculations for molecule-metal interfaces using a substrate screening approach. *Journal of Chemical Theory and Computation* **2019**, *15*, 4218–4227.
- (57) Klüner, T.; Govind, N.; Wang, Y. A.; Carter, E. A. Periodic density functional embedding theory for complete active space self-consistent field and configuration interaction calculations: Ground and excited states. *The Journal of chemical physics* **2002**, *116*, 42–54.
- (58) Lahav, D.; Klüner, T. A self-consistent density based embedding scheme applied to the adsorption of CO on Pd (111). *Journal of Physics: Condensed Matter* **2007**, *19*, 226001.
- (59) Zhu, T.; Cui, Z.-H.; Chan, G. K.-L. Efficient formulation of ab initio quantum embedding in periodic systems: Dynamical mean-field theory. *Journal of Chemical Theory and Computation* **2019**, *16*, 141–153.
- (60) Zhu, T.; Chan, G. K.-L. Ab Initio Full Cell G W+ DMFT for Correlated Materials. *Physical Review X* **2021**, *11*, 021006.
- (61) Chan, G. K.-L.; Sharma, S. The density matrix renormalization group in quantum chemistry. *Annual Review of Physical Chemistry* **2011**, *62*, 465–481.

- (62) Knizia, G.; Chan, G. K.-L. Density matrix embedding: A simple alternative to dynamical mean-field theory. *Physical review letters* **2012**, *109*, 186404.
- (63) Mehdaoui, I.; Klüner, T. Understanding surface photochemistry from first principles: The case of CO-NiO (100). *Physical review letters* **2007**, *98*, 037601.
- (64) Martirez, J. M. P.; Carter, E. A. Prediction of a low-temperature N₂ dissociation catalyst exploiting near-IR-to-visible light nanoplasmonics. *Science advances* **2017**, *3*, eaao4710.
- (65) Jin, Z.; Subotnik, J. E. Nonadiabatic dynamics at metal surfaces: fewest switches surface hopping with electronic relaxation. *Journal of Chemical Theory and Computation* **2021**, *17*, 614–626.
- (66) Subotnik, J. E.; Yeganeh, S.; Cave, R. J.; Ratner, M. A. Constructing diabatic states from adiabatic states: Extending generalized Mulliken–Hush to multiple charge centers with Boys localization. *The Journal of chemical physics* **2008**, *129*, 244101.
- (67) Subotnik, J. E.; Cave, R. J.; Steele, R. P.; Shenvi, N. The initial and final states of electron and energy transfer processes: Diabatization as motivated by system-solvent interactions. *The Journal of chemical physics* **2009**, *130*, 234102.
- (68) Chen, J.; Dou, W.; Subotnik, J. Active Spaces and Non-Orthogonal Configuration Interaction Approaches for Investigating Molecules on Metal Surfaces. *Journal of Chemical Theory and Computation* **2022**,
- (69) Glover, W. Communication: Smoothing out excited-state dynamics: Analytical gradients for dynamically weighted complete active space self-consistent field. *The Journal of Chemical Physics* **2014**, *141*, 171102.
- (70) Battaglia, S.; Lindh, R. Extended dynamically weighted CASPT2: The best of two worlds. *Journal of chemical theory and computation* **2020**, *16*, 1555–1567.

- (71) Chen, J.; Subotnik, J. (unpublished).
- (72) Bulla, R.; Costi, T. A.; Pruschke, T. Numerical renormalization group method for quantum impurity systems. *Reviews of Modern Physics* **2008**, *80*, 395.
- (73) Dou, W.; Miao, G.; Subotnik, J. E. Born-oppenheimer dynamics, electronic friction, and the inclusion of electron-electron interactions. *Physical Review Letters* **2017**, *119*, 046001.
- (74) If we parametrize $x = \langle d|t \rangle$, $y = \langle d|u \rangle$, then we have three equations (1 coming from Eq. 3 and 2 coming from Eq. 5) to solve three variables x, y and θ .
- (75) If we parametrize $x = \langle d_1|t \rangle$, $y = \langle d_1|u \rangle$, $z = \langle d_2|t \rangle$, $w = \langle d_2|u \rangle$ and it will be three equations solving 5 variables x, y, z, w and θ .
- (76) Peng, W.-T.; Fales, B. S.; Shu, Y.; Levine, B. G. Dynamics of recombination via conical intersection in a semiconductor nanocrystal. *Chemical Science* **2018**, *9*, 681–687.
- (77) Smith, J. E.; Lee, J.; Sharma, S. Near-exact nuclear gradients of complete active space self-consistent field wave functions. *The Journal of Chemical Physics* **2022**, *157*, 094104.